

# 2 Application of nuclear inelastic scattering 3 spectroscopy to the frequency scale calibration of *ab* 4 *initio* calculated phonon density of states of 5 quasi-one-dimensional iron ternary chalcogenides

6 Airat Kiiamov<sup>1,\*</sup>, Vladimir Tsurkan<sup>2,3</sup>, Dorina Croitori<sup>2</sup>, Hans-Albrecht Krug von Nidda<sup>3</sup>, Zakir  
7 Seidov<sup>3,4</sup>, Hans-Christian Wille<sup>5</sup>, Ilya Sergueev<sup>5</sup>, Olaf Leupold<sup>5</sup>, Dmitrii Tayurskii<sup>1</sup>, and Lenar  
8 Tagirov<sup>1,6</sup>

9 <sup>1</sup> Institute of Physics, Kazan Federal University, 420008 Kazan, Russia

10 <sup>2</sup> Institute of Applied Physics, MD-20208 Chisinau, Moldova

11 <sup>3</sup> Experimental Physics V, Center for Electronic Correlations and Magnetism, Institute of Physics, University  
12 of Augsburg, D-86135 Augsburg, Germany

13 <sup>4</sup> Institute of Physics, Azerbaijan National Academy of Sciences, AZ-1143 Baku, Azerbaijan

14 <sup>5</sup> Deutsches Elektronen-Synchrotron DESY, D-22607 Hamburg, Germany

15 <sup>6</sup> Zavoisky Physical-Technical Institute, FRC Kazan Scientific Center of RAS, 420029 Kazan, Russia

16

17 \* Correspondence: AiratPhD@gmail.com; Tel.: +7-967-360-5499

18

Received: date; Accepted: date; Published: date

19 **Abstract:** This study aims to examine the applicability of nuclear inelastic scattering (NIS) and  
20 conventional Mössbauer spectroscopy for calibration of the frequency scale of *ab initio* calculated  
21 phonon density of states (PDOS) of iron ternary chalcogenides. NIS measurements are carried out  
22 on the quasi-one-dimensional ternary chalcogenide RbFeSe<sub>2</sub> to obtain the partial PDOS of the iron  
23 atoms in the compound. We compare the experimental PDOS with our previous results on  
24 vibrational properties of RbFeSe<sub>2</sub> obtained with DFT *ab initio* calculations, conventional Mössbauer,  
25 and infra-red spectroscopies. The experimental PDOS measured by NIS is collated with the *ab initio*  
26 calculated one. The frequency correction factor for the *ab initio* results is determined as 1.077 in  
27 good agreement with value of 1.08 obtained previously from the temperature dependence of the  
28 Lamb-Mössbauer factor of the iron atoms in RbFeSe<sub>2</sub>. We conclude that nuclear inelastic scattering  
29 and temperature dependence of the Lamb-Mössbauer factor in conventional Mössbauer  
30 spectroscopy can be equally applied for evaluation of the frequency correction factor for *ab initio*  
31 calculated phonon density of iron of ternary chalcogenides.

32 **Keywords:** nuclear inelastic scattering; phonon density of states; *ab initio* DFT theory; DFT phonon  
33 frequency correction factor  
34

---

## 35 1. Introduction

36 Undoubtedly, specific heat is one of the most informative features of a solid. The temperature  
37 dependence of the specific heat of solids enables the detection of any type of phase transition of  
38 different origin. Hence, specific-heat investigations are quite useful in studies of complex magnetic  
39 systems, see [1] for instance. The correctness of an anticipated spin-Hamiltonian and corresponding  
40 approximations to describe a certain magnetic system can be checked by comparison of the  
41 experimental specific-heat data with the theoretical predictions derived from the model (see, for  
42 example, Ref.[2]). Such comparison also allows resolving of various ambiguities in the description of  
43 complex magnets. For example, the difference of magnon dispersions in antiferromagnets and  
44 ferromagnets manifests itself in the temperature dependences of the magnetic contribution to the  
45 specific heat. Such difference allows us e.g. to discern a pure ferromagnetic state and an

46 antiferromagnet state with unequal magnetic moments on different magnetic sub-lattices. Moreover,  
47 the magnetic contribution to the specific heat allows estimating the entropy of the magnetic  
48 sub-system of corresponding solids, and the temperature dependence of the magnetic entropy  
49 enables the determination of the spin state of ions in solids with the long-range magnetic order (see,  
50 for example, [3]). So, one can argue that the temperature dependences of the magnetic specific heat  
51 and the magnetic entropy of new and complex magnetic systems are essential for their full and  
52 consistent theoretical description.

53 The specific heat of a magnetic sub-system of a compound can be determined as the difference  
54 of the total specific heat and all contributions of non-magnetic origin such as lattice, electronic,  
55 two-level centers, and possible others. In the case of dielectrics, the temperature dependence of the  
56 lattice specific heat allows us to determine precisely the magnetic specific heat.

57 At low temperatures, the lattice specific heat of solids can be adequately described in terms of  
58 the Debye model [4]. However, with increasing temperature, the occupancy of the high-energy  
59 phonon modes increases [3]. This demands the extension of the Debye approximation by adding a  
60 set of additional contributions based on the Einstein model [4,5]. The correctness of such approaches  
61 is highly dependent on the used parameters such as Debye and Einstein temperatures and the  
62 number of modes, which are usually determined empirically. Moreover, in the case of solids with a  
63 large number of optical phonon modes, that is typical for the low-symmetry crystal structures, the  
64 number of Einstein modes can be unreasonably numerous. So, one can argue that for the  
65 specific-heat approximation such a classical approach can be reasonably used only at low  
66 temperatures when most of the optical oscillation modes are not occupied.

67 Thus, in the case of solids with relatively high magnetic-ordering temperatures, it is necessary  
68 to use other approaches [3]. To date, new *ab initio* methods for calculating the lattice contribution to  
69 the heat capacity have proven themselves well. Based on the density functional theory (DFT), these  
70 *ab initio* methods provide calculating the total and partial phonon density of states (PDOS) for a solid  
71 by using only the information about its crystal structure and chemical composition. Modern  
72 crystallographic investigation methods provide respectable accuracy for measuring the  
73 crystal-structure parameters and stoichiometry of solids. In its turn, the phonon density of states  
74 enables us to calculate the lattice contribution to the specific heat directly by using the harmonic  
75 approximation [6]. Apparently, this makes such an *ab initio* way for specific-heat calculations  
76 independent of the empirical parameters. Nevertheless, a feature of DFT does not allow us to call  
77 such an approach to be fully independent on empirical parameters. It is well known that a  
78 systematic overestimation of the atomic binding energies and lattice constants is inherent for the  
79 DFT calculations [7, 8]. It leads to inaccuracy of the estimation of the eigenfrequencies of the phonon  
80 modes. The accurate quantitative estimation of the temperature dependence of the lattice specific  
81 heat by the PDOS needs a preliminary correction of its frequency scale. In the case of systematic  
82 underestimation of the force values, the frequency scale can be corrected by multiplying the  
83 frequencies of all phonon modes by a single parameter, *i.e.* the frequency correction factor [3].

84 There are different ways to determine the correction factor. For instance, Raman and infrared  
85 (IR) spectroscopy enable measuring the oscillation frequencies for Raman and IR-active phonon  
86 modes, respectively [2]. To a first approximation, the IR-active phonon oscillation frequency should  
87 coincide with the IR absorption peak [3]. Therefore, a comparison of the calculated PDOS with the  
88 measured IR-absorption spectrum enables estimating the frequency correction factor for any solid  
89 with IR-active phonon modes. Nevertheless, such a way for estimation does not take into account  
90 the oscillator strength of the phonon modes. In the case of IR-absorption maxima of different phonon  
91 modes overlaying each other in the IR-spectrum, neglecting the oscillator strengths leads to possible  
92 errors of the phonon-mode frequency estimation.

93 In the case of an iron-containing solid,  $^{57}\text{Fe}$  Mössbauer spectroscopy methods also allow the  
94 estimation of the frequency correction factor (generally, the statement refers to a solid containing  
95 any kind of Mössbauer nuclei, which are not rare in the periodic table of elements, but only a few  
96 isotopes are suitable for practical application [9]). The Mössbauer effect is the resonant and recoilless

97 absorption of gamma radiation by atomic nuclei bound into a solid. The probability of the effect is  
98 called Lamb-Mössbauer factor [9]. It depends on the mean-square displacement of a nucleus, the  
99 temperature dependence of which is determined directly by the partial PDOS of the corresponding  
100 atom [9]. Besides, the Lamb-Mössbauer factor can be estimated as the relative total area under the  
101 Mössbauer spectrum [9]. So, the temperature dependence of the Lamb-Mössbauer factor can be  
102 obtained by measuring Mössbauer spectra at different temperatures. On the other hand, it can be  
103 modeled by calculating the partial PDOS of the corresponding atom. Hence, the comparison of the  
104 experimental and calculated temperature dependences of the Lamb-Mössbauer factor yields another  
105 estimate of the correction factor for the PDOS frequency. In our previous paper [3], we used both  
106 these approaches to estimate the frequency correction factor for the *ab initio* calculated PDOS of the  
107 quasi 1D antiferromagnet RbFeSe<sub>2</sub>. The value of 1.06 had been obtained from the comparison of the  
108 high-frequency IR absorption peak frequencies with those in the calculated PDOS, while the fit to  
109 the temperature dependence of the Lamb-Mössbauer factor had given the value of 1.08.

110 The approach to fit the temperature dependence of the Lamb-Mössbauer factor is quite indirect  
111 compared with the IR-spectroscopy method mentioned above, although the latter one cannot be  
112 regarded as absolutely accurate because of difficulties with determining the oscillator strengths. To  
113 resolve the dilemma of choosing one of the two methods, another experimental method to measure  
114 the PDOS is strongly desired.

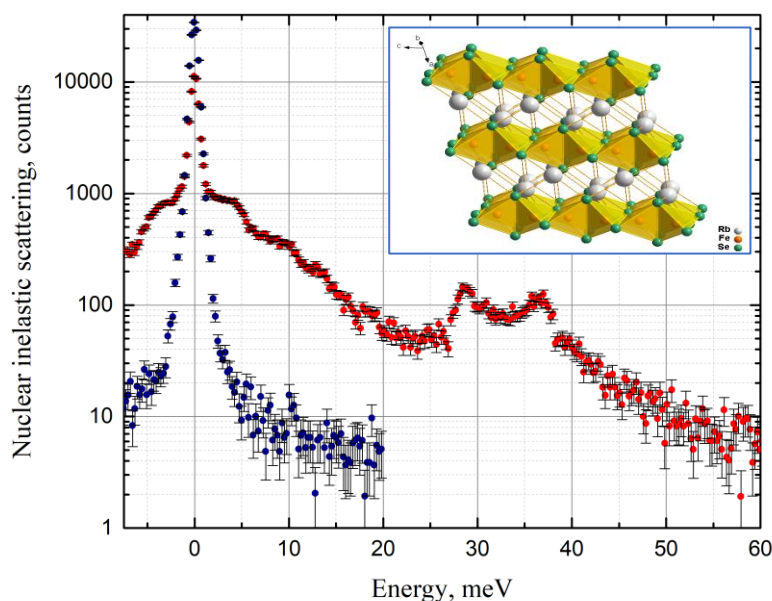
115 There are several methods to measure the PDOS in solids. Widely known is inelastic neutron  
116 scattering (INS), the advantage of which is its universality [10]. On the other hand, it is quite  
117 laborious and requires a large amount of sample, typically several dozens of grams, because of the  
118 small scattering cross-section of neutrons in solids. Another one is the nuclear inelastic scattering  
119 (NIS) method [11,12], which is based on the Mössbauer effect, utilizing synchrotron radiation. It is  
120 not universal as INS, since it can be applied only for a solid containing a resonant nucleus, like <sup>57</sup>Fe,  
121 similar to conventional Mössbauer spectroscopy. The advantages of the NIS method are as follows:  
122 it requires significantly less sample than INS (typically below 0.5 gram); it is much less laborious  
123 (takes several hours for one run); the outcome is just the partial PDOS for the kind of atoms the  
124 resonant nucleus of which is probed. It is iron in the case of <sup>57</sup>Fe resonant nuclei. The compound we  
125 study is RbFeSe<sub>2</sub> that makes NIS a suitable technique to obtain its PDOS and to utilize the NIS data  
126 to calibrate the frequency scale of our *ab initio* calculation of the PDOS for this compound.

127 The objectives of this paper are as follows: (i) to measure the partial iron PDOS of RbFeSe<sub>2</sub> by  
128 NIS method, (ii) to compare the calculated partial PDOS with the measured one in order to  
129 determine the frequency correction factor and to check the correctness of the computed results; (iii)  
130 to compare the correction factor obtained in the present paper with those which we previously got  
131 from the analysis of the IR-absorption spectrum and the temperature dependence of the  
132 Lamb-Mössbauer factor; (iv) to draw a conclusion on the applicability of these indirect, IR and  
133 Lamb-Mössbauer, methods for the calibration of the frequency scale for the *ab initio* calculated PDOS  
134 of a solid. A more general implication concerns checking the quantitative accuracy of *ab initio* density  
135 functional theory (DFT) calculations of the PDOS in quasi-one-dimensional ternary compounds.  
136

## 137 2. Experimental details and results

138 The nuclear inelastic scattering [11,12] experiment was carried out at the Dynamics Beamline  
139 P01 of PETRA III synchrotron (DESY, Hamburg, Germany) [13]. The measurements utilizing the  
140 nuclear gamma-resonance of <sup>57</sup>Fe at 14.413 keV were performed with an inline high-resolution  
141 monochromator providing an energy bandwidth of 0.9 meV full width at half maximum (FWHM).  
142 The sample with natural enrichment by <sup>57</sup>Fe was measured at 295 K. The Fe NIS spectrum of RbFeSe<sub>2</sub>  
143 is shown in Figure 1 (red dots) along with the instrumental function measured simultaneously with  
144 the spectrum (blue dots in Fig.1).

145 The partial iron PDOS was evaluated from the NIS spectrum using the procedure described in  
 146 Ref. [14]. The partial PDOS for the iron atoms in RbFeSe<sub>2</sub> is shown in Figure 2 (black dots).



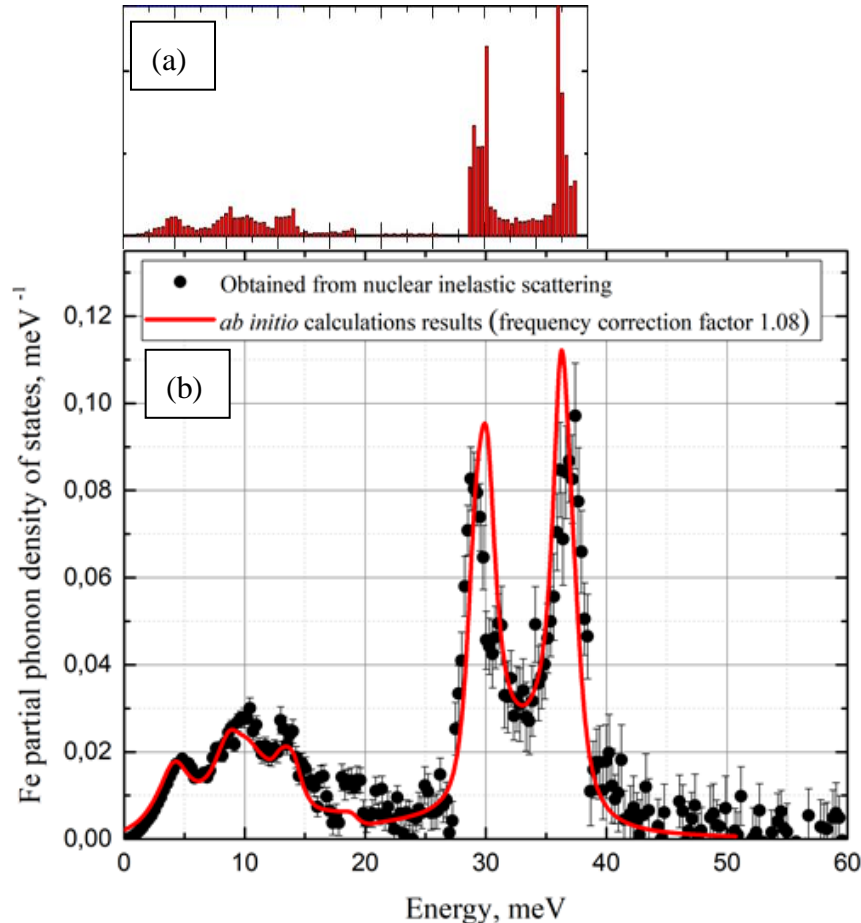
147  
 148 **Figure 1.** <sup>57</sup>Fe nuclear inelastic scattering spectrum of RbFeSe<sub>2</sub> (red dots) and instrumental function (blue dots).  
 149 The inset displays a fragment of the RbFeSe<sub>2</sub> crystal structure showing quasi-one-dimensional structure of  
 150 edge-sharing [FeSe<sub>4</sub>] tetrahedra.

151 The *ab initio* calculations were carried out within the framework of density functional theory (DFT)  
 152 utilizing the Vienna *ab-initio* simulation package (VASP 5.3) [15–18]. The Perdew–Burke–Ernzerhof  
 153 (PBE) generalized gradient approximation (GGA) was applied for the exchange and correlation  
 154 corrections [19]. The projector-augmented wave (PAW) method is used to take into account the  
 155 electron-ion interactions. The PAW method is a frozen-core one in which the valence Rb (4p<sup>6</sup> 5s<sup>1</sup>),  
 156 Fe (3d<sup>6</sup> 4s<sup>2</sup>), Se (4s<sup>2</sup> 4p<sup>4</sup>) electrons are treated explicitly, while the remaining electrons of the cores  
 157 are taken into account by using pseudopotentials [20]. The cutoff energy for the plane-wave basis  
 158 set was selected 300 eV. Integration over the Brillouin zone had been done on a Monkhorst–Pack k-point  
 159 mesh 3×2×3 which corresponds to the actual spacing of 0.300×0.259×0.202 per Å [21]. Equilibrium  
 160 geometry was obtained after the several stages of full structural relaxation that include atomic  
 161 positions, cell shape and cell volume. The phonon dispersion and density of states (PDOS) were  
 162 obtained within harmonic approximation making use of the Medea-Phonon software [6]. The  
 163 approach to the lattice dynamics is based on the *ab-initio* evaluation of forces acting on all atoms by  
 164 a set of finite displacements of a few atoms within an otherwise perfect crystal. The lattice  
 165 parameters obtained after the lattice relaxation are given by  $a = 7.520$  Å,  $b = 12.153$  Å,  $c = 5.574$  Å,  
 166 and the angle  $\beta = 111.83^\circ$ . There is a slight deviation of the calculated lattice parameters from the  
 167 experimental ones [5] of about 1–2 percent is typical for DFT calculations [2].

168 All calculations accounted for the spin polarization due to the antiferromagnetic ordering of  
 169 RbFeSe<sub>2</sub>. The antiferromagnetic spin pattern was set in accordance with the magnetic structure  
 170 obtained previously by neutron diffraction data [22]. The best agreement between the calculated  
 171 ( $m(\text{Fe}) = 2.80$  μB) and the experimental ( $m(\text{Fe}) = 2.66$  μB [22,23]) values of the magnetic moment per  
 172 iron ion was obtained for choosing the Hubbard  $U$  parameter equal to zero.

173 The red colored histogram in Fig. 1a shows PDOS which is output of *ab-initio* calculations [3]  
 174 with the calibrated frequency scale (see below). The solid red line in Fig. 2b shows the calibrated (cf.  
 175 Section 3) partial PDOS for the iron atoms obtained from the previously calculated *ab initio* one,

176 Fig. 2a. The calculated PDOS is a discrete set of contributions from phonon modes, while the  
 177 experimental one is a quasi-continuous sequence determined by the settings of the beamline setup,  
 178 but to the greatest extent by the monochromator energy (frequency) resolution of 0.9 meV. To  
 179 compare the experiment with the *ab initio* calculated iron partial PDOS the latter was convoluted  
 180 with a Gaussian profile with an FWHM of 0.9 meV matching the resolution window of the  
 181 monochromator. The result of the convolution is just the solid red line presented in Fig. 2b.



189

190 **Figure 2.** (a) Calculated PDOS for iron ions in RbFeSe<sub>2</sub> [3] (*ЛТ – предлагаю дать в одинаковой шкале по*  
 191 *абсциссе – дополнить правую, нулевую часть, заодно будет отличаться от Физрева*); (b) Partial PDOS  
 192 for iron atoms of RbFeSe<sub>2</sub> obtained from the nuclear inelastic scattering spectrum (black dots) and  
 193 from the *ab initio* PDOS smoothen by the Gaussian profile (red line, see description in the body text).

### 194 3. Discussion

195 The experimental iron partial PDOS of RbFeSe<sub>2</sub> shows a quite complex dependence on the  
 196 energy of oscillations with numerous maxima (Fig. 2). It is essentially of non-Debye type if we  
 197 consider the full frequency range of possible lattice vibrations. It shows a parabolic increase with the  
 198 energy, as prescribed by the conventional Debye model, only at small energies up to approximately  
 199 ~ 4 meV (~ 45 K). This is quite expectable, given the low-symmetry chain-like crystal structure and  
 200 complex unit cell of the compound, while the Debye model considers acoustic vibrations in an  
 201 isotropic three dimensional solid and works well if the measurement temperature is significantly  
 202 below the Debye temperature.

203 To interpret the specific-heat measurements for RbFeSe<sub>2</sub> in the temperature range 2-296 K in a  
 204 first approach [5] we previously combined the Debye contribution with the Einstein contributions,  
 205 and the more Einstein modes we included in the model, the better was the fit of the experimental  
 206 data. Simultaneously, the magnetic contribution to the total entropy change from 2 K to 296 K fell

207 down below 10% of the minimal value confined to  $S = \frac{1}{2}$  spin-state of the iron ion, which is not  
208 reasonable. Our study revealed that the phenomenological description of the temperature  
209 dependence of the heat capacity of the chain iron chalcogenides is not constructive, not only because  
210 of the strongly non-Debye type of the PDOS, Fig. 2, but also due to the inability of calibrating the  
211 absolute value of the lattice contribution to the heat capacity (the entropy, in fact), without which it  
212 is impossible to separate quantitatively the magnetic contribution to the heat capacity from the  
213 lattice one.

214 In continuation of our studies [3], the *ab-initio* approach allowed to calculate the lattice specific  
215 heat of RbFeSe<sub>2</sub> formally without adjustable parameters, because it is based on exact counting of  
216 vibrational eigenmodes, acoustical and optical. However, as it was mentioned above, the DFT  
217 underestimates the eigenfrequencies of the phonon modes. The frequency scale correction is one of  
218 the simplest ways of calibration, but the working approach and the accurate procedure of finding  
219 the correction factor becomes crucial.

220 Figure 2 shows good agreement between the *ab initio* calculated PDOS and the PDOS evaluated  
221 from our NIS data. The calculated pattern quantitatively describes all features of the iron PDOS  
222 within the entire frequency range of vibrations in the RbFeSe<sub>2</sub> lattice. The value of the frequency  
223 correction factor corresponding to the best fit of the *ab initio* calculated pattern to the experimental  
224 one is 1.077. That value is practically identical to that obtained previously with the Lamb- Mössbauer  
225 factor temperature dependence (1.08). Such accordance confirms the correctness of our previous  
226 results and shows that the temperature dependence of the Lamb-Mössbauer factor can be used for  
227 accurate calibration of the results of *ab initio* calculations of vibrational properties of solids.

#### 228 4. Summary and conclusion

229 We presented the results of <sup>57</sup>Fe nuclear inelastic scattering measurements of the  
230 quasi-one-dimensional antiferromagnet RbFeSe<sub>2</sub>. The outcome of the NIS spectrum is the partial  
231 PDOS of the iron atoms. The experimentally evaluated partial PDOS was directly compared with the  
232 partial PDOS of iron atoms calculated utilizing the DFT *ab initio* method. The comparison has shown  
233 good quantitative agreement between the calculated and the experimentally measured partial PDOS  
234 of iron atoms in RbFeSe<sub>2</sub> and allowed us to determinate the frequency correction factor for the DFT  
235 partial PDOS as  $\sim 1.077 (\pm 0.002)$ . This correction factor appeared to be practically equal to the  
236 frequency correction factor of  $\sim 1.08$  obtained from the fitting of the temperature dependence of the  
237 Lamb-Mössbauer factor in conventional Mössbauer spectroscopy. Thus, both techniques can be  
238 equally applied for evaluation of the frequency correction factor for the DFT PDOS subject to  
239 availability.

240 The frequency correction factor for DFT partial PDOS calculations has indisputable  
241 implications on rectifying the magnetic contribution to the specific heat and the change of magnetic  
242 entropy upon the transition from the nominally ordered antiferromagnetic state at lowest  
243 temperatures of measurements to the high-temperature disordered paramagnetic state of magnetic  
244 ions in quasi-one-dimensional compounds. DFT *ab initio* calculations of strongly non-Debye  
245 vibrational properties complemented with an instrumental evaluation of the frequency correction  
246 factor constitute a modern approach to the quantitative analysis of thermal properties of systems  
247 with reduced dimensionality.

248

249 **Author Contributions:** Conceptualization, A.K. and D.T.; methodology, A.K., L.T., and I.S.; sample  
250 preparation, V.T. and D.C.; formal analysis, A.K. and I.S.; investigation, A.K., V.T. and I.S.; resources, D.C., V.T.,  
251 H.-A.KvN. and Z.S.; data curation, A.K., I.S., H.-C.W. and O.L.; writing—original draft preparation, A.K.;  
252 writing—review and editing, H.-A.KvN., A.K. and L.T.; visualization, A.K.; supervision, L.T.; project  
253 administration, D.T. and H.-A.KvN.; funding acquisition, D.T. and H.-A.KvN. All authors have read and  
254 agreed to the published version of the manuscript.

255 **Funding:** The reported study was funded by RFBR and DFG according to research projects №19-51-45001 and  
256 KR2254/3-1.

257 **Conflicts of Interest:** The authors declare no conflict of interest.

258

## 259 References

- 260 1. Fu, H.H.; Yao, K.L.; Liu, Z.L. Specific heat study on a spin-one-half frustrated diamond chain.  
261 *Physics Letters A* **2006**, *358*, 443–447.
- 262 2. Lysogorskiy, Y.V.; Eremina, R.M.; Gavrilova, T.P.; Nedopekin, O.V.; Tayurskii, D.A. Vibrational  
263 and magnetic properties of crystalline CuTe<sub>2</sub>O<sub>5</sub>. *JETP Letters* **2015**, *100*, 652–656.
- 264 3. Kiiamov, A.G.; Lysogorskiy, Y.V.; Vagizov, F.G.; Tagirov, L.R.; Tayurskii, D.A.; Seidov, Z.;  
265 Krug von Nidda, H.-A.; Tsurkan, V.; Croitoro, D.; Günther, A.; Mayr, F.; Loidl, A. Vibrational  
266 properties and magnetic specific heat of the covalent chain antiferromagnet RbFeSe<sub>2</sub>. *Phys. Rev.*  
267 *B* **2018**, *98*, 214411.
- 268 4. Kittel, Ch. *Introduction to Solid State Physics*, 7<sup>th</sup> ed.; John Wiley & Sons, Inc. 1996, Chapter 5.
- 269 5. Seidov, Z.; Krug von Nidda, H.-A.; Tsurkan, V.; Filippova, I.G.; Günther, A.; Gavrilova, T.P.;  
270 Vagizov, F.G.; Kiiamov, A.G.; Tagirov, L.R.; Loidl A. Magnetic properties of the covalent chain  
271 antiferromagnet RbFeSe<sub>2</sub>. *Phys. Rev. B* **2016**, *94*, 134414.
- 272 6. Parlinski, K.; Li, Z.; Kawazoe, Y. First-Principles Determination of the Soft Mode in Cubic ZrO<sub>2</sub>.  
273 *Phys. Rev. Lett.* **1997**, *78*, 4063.
- 274 7. Braïda, B.; Hiberty, P.C.; Savin, A.A. Systematic Failing of Current Density Functionals:  
275 Overestimation of Two-Center Three-Electron Bonding Energies. *J. Phys. Chem. A* **1998**, *102*,  
276 7872–7877.
- 277 8. Grinberg, I.; Ramer, N.J.; Rappe, A.M. Quantitative criteria for transferable pseudopotentials in  
278 density functional theory. *Phys. Rev. B* **2001**, *63*, 201102(R).
- 279 9. Gütlich, Ph.; Bill, E.; Trautwein, A. X. *Mössbauer Spectroscopy and Transition Metal Chemistry.*  
280 *Fundamentals and Applications*, 1st ed.; Springer-Verlag: Berlin, Germany, 2011; pp. 7–24.
- 281 10. Dorner, B. *Coherent Inelastic Neutron Scattering in Lattice Dynamics*; Springer Tracts in Modern  
282 Physics v.93, Springer-Verlag: Berlin Heidelberg New York, 1982; 102 p.
- 283 11. Chumakov, A.; Ruffer, R. Nuclear inelastic scattering. *Hyperfine Interact.* **1998**, *113*, 59–79.  
284 <https://doi.org/10.1023/A:1012659229533>
- 285 12. Ruffer, R.; Chumakov, A.I. Nuclear inelastic scattering. *Hyperfine Interact.* **2000**, *128*, 255–272.  
286 <https://doi.org/10.1023/A:1012643918108>
- 287 13. Wille, H.-C.; Franz, H.; Röhlberger, R.; Caliebe, W. A.; Dill, F.-U. Nuclear resonant scattering at  
288 PETRA III : Brilliant opportunities for nano- and extreme condition science. *J. Phys.: Conf.*  
289 *Ser.* **2009**, *217*, 012008.
- 290 14. Kohn, V.G.; Chumakov, A.I. DOS: Evaluation of phonon density of states from nuclear resonant  
291 inelastic absorption. *Hyperfine Interact.* **2000**, *125*, 205–221.
- 292 15. G. Kresse and J. Hafner, *Phys. Rev. B* **1993**, *47*, 558.
- 293 16. G. Kresse and J. Hafner, *Phys. Rev. B* **1994**, *49*, 14251.
- 294 17. G. Kresse and J. Furthmuller, *Comput. Mater. Sci.* **1996**, *6*, 15.
- 295 18. G. Kresse and J. Furthmuller, *Phys. Rev. B* **1996**, *54*, 11169.
- 296 19. J.P. Perdew, K. Burke, and M. Ernzerhof, *Phys. Rev. Lett.* **1996**, *77*, 3865.
- 297 20. P.E. Blöchl, *Phys. Rev. B* **1994**, *50*, 17953.
- 298 21. H.J. Monkhorst and J.D. Pack, *Phys. Rev. B* **1976**, *13*, 5188.
- 299 22. Bronger, W.; Kyas, A.; Müller, P. The antiferromagnetic structures of KFeS<sub>2</sub>, RbFeS<sub>2</sub>, KFeSe<sub>2</sub>,  
300 and RbFeSe<sub>2</sub> and the correlation between magnetic moments and crystal field calculations. *J.*  
301 *Solid State Chem.* **1987**, *70*, 262–270.

302 23. Bronger, W.; Müller, P. The magnetochemical characterisation of the bonding features in  
303 ternary chalcogenides of manganese, iron and cobalt with low dimensional structural units. *J.*  
304 *Alloys Compd.* **1997**, *246*, 27-36.

305 The magnetochemical characterisation of the bonding features in ternary chalcogenides of  
306 manganese, iron and cobalt with low dimensional structural units

307  
308



© 2020 by the authors. Submitted for possible open access publication under the terms and conditions of the Creative Commons Attribution (CC BY) license (<http://creativecommons.org/licenses/by/4.0/>).

309

310